CWE-8
June 7-11, 2026
London, ON, Canada

Influence of crown porosity on drag coefficient of deciduous and coniferous model trees

A. Awol [a], M. N. Owais [b], G. T. Bitsuamlak [c], K. Siddiqui [d]

[a,b,c,d] *WindEEE Research Facility, University of Western Ontario, London, Ontario, Canada, ademsis@uwo.ca, mowais@uwo.ca, gbitsuam@uwo.ca, ksiddiq@uwo.ca*

SUMMARY

Trees play a significant role in regulating the urban microclimate through complex multiphysics interactions. A thorough understanding of turbulent airflow around urban trees is essential for assessing the outdoor thermal comfort, pedestrian-level wind conditions, building energy performance, and urban heat island mitigation. Unlike conventional structures, trees exhibit distinct aerodynamic behavior in urban microclimate studies due to their porous foliage and structural flexibility. The current study investigates the aerodynamic characteristics of scaled deciduous and coniferous trees using artificial tree models with varying porosities and wind conditions at WindEEE Dome, a large multiscale wind testing facility. The results show a negative sloped relationship between the drag coefficient C_d and crown porosities at a given wind speed U for both configurations. The C_d increases and then decreases with wind speed in the deciduous tree model, indicating the reconfiguration of branches at different speeds. For the coniferous tree model, relatively higher C_d values are observed and at higher wind speeds, the drag coefficient exhibits nearly invariant behaviour with increasing wind speed.

Keywords: *WindEEE, aerodynamics, wind tunnel, urban microclimate, Coniferous, Deciduous, drag, trees*

1. INTRODUCTION

Rapid urbanization significantly contributes to the global climate change by increasing Greenhouse Gas (GHG) emissions (through increased energy consumption) and reducing green spaces. Urban densification and high-rise buildings restrict wind flow, elevate air temperatures, and reduce outdoor thermal comfort. The Urban microclimates (UMC) is governed by complex interactions involving solar radiation, heat storage and release from surfaces, wind-driven convection, vegetation evapotranspiration, and anthropogenic heat sources (Zhao, 2023). It is predicted that nearly 70% of the world population will be living in urban areas by 2050, increasing the risk of extreme heat events such as the Urban Heat Island (UHI) effect (Wang et al., 2021).

Trees play a vital role in improving local microclimate by mitigating the adverse effects of the UHI (Manickathan et al., 2018). The flexible and porous nature of trees enables them to absorb more momentum than solid obstacles, producing extended wakes compared to impermeable structures (Gromke and Ruck, 2008; Grant and Nickling, 1998). Trees also possess a high surface-to-volume ratio, resulting in significant skin friction and aerodynamic resistance around foliage, making skin friction a non-negligible component of the total drag force (Raupach, 1992; Finnigan, 2000). This contrasts with bluff bodies, where drag is dominated by pressure differences between windward and leeward sides (Gromke and Ruck, 2008), (Zhao et al., 2023). Cao et al. (2012) demonstrated that aerodynamic behavior is influenced not only by reconfiguration but also by upstream turbulence and crown streamlining. Mochida et al. (2008) and Mochida and Lun (2008) demonstrated that the aerodynamic effects of trees reduce mean wind velocity while enhancing turbulence. In UMC, these aerodynamic effects strongly influence near-ground wind flow, turbulence generation, and momentum exchange within street canyons and open urban spaces

(Oke, 1988). As a result, urban trees affect ventilation efficiency, pollutant dispersion, and pedestrian thermal comfort (Gromke et al., 2008; Buccolieri et al., 2011). Moreover, trees enhance outdoor thermal comfort by regulating temperature through shading and evapotranspiration, improving air quality, and supporting urban biodiversity (Buccolieri et al., 2011).Three approaches are commonly used to study vegetation impact on the microclimate: (1) Field measurements, (2) Numerical simulations, and (3) Wind tunnel experiments (Manickathan et al., 2018).

Field measurements have limitations of restricted spatial coverage, coarse spatial resolution, and uncontrollable environmental conditions, but they are primarily used to validate numerical models. CFD simulations often struggle to accurately represent complex wake flows caused by tree flexibility and reconfiguration. Wind tunnel experiments, while subject to increased cost and challenge of achieving all similarity requirements simultaneously, provide a controlled environment to investigate airflow around trees. The use of an Atmospheric Boundary Layer (ABL) profile in wind tunnel studies enables a realistic investigation of trees in urban environments (Gromke, 2011). The similarity criteria must be satisfied to relate wind tunnel experiment findings to full-scale conditions . The scaling of large natural trees to small artificial models presents challenges, particularly in representing reconfiguration, deformation, and vibration, which strongly influence drag and wake flow characteristics (Manickathan et al., 2018).

The current study investigates the aerodynamic characteristics of scaled isolated deciduous and coniferous trees using artificial tree models. Each tree model is configured with five varying crown porosities in an ABL wind tunnel representing open and smooth terrain exposures. The results of this study will improve the understanding of tree aerodynamics by providing important data for large scale trees with the ability of reconfiguration under wind flow.

2. METHODOLGOY

2.1. Experimental setup

The experimental study is conducted at the Wind Engineering, Energy and Environment Research Facility (WindEEE RF) at Western University, Canada. It is the first $3D$ wind chamber, featuring a hexagonal test section with a $25m$ diameter. A total of 106 individually controlled fans, installed along the peripheral walls and ceiling, along with 202 louver systems, enable precise control of wind flow. The test is conducted in a straight flow closed loop, utilizing one wall of 60 fans (4 high x 15 wide). The test section is $14m$ wide, $25m$ long and $3.8m$ high.

Two tree models of equal height of $h = 0.603m$ are used for testing. The coniferous tree model is represented by a $1{:}\,25$ scaled Cedar tree while a $1{:}\,10$ scaled Lemon tree model is used to represent the deciduous tree. Each tree model is configured with five crown porosities, ranging from full foliage to defoliated conditions, in an ABL wind tunnel corresponding to open and smooth terrain exposures. These models are selected due to their ability to modify crown porosity, unlike commonly used rigid tree models. The tree models are thinned by reducing the canopy through systematically removing selected branches to observe the variation in the crown porosities. A force balance, $JR3\ 30E$ multi-axis Force-Torque Sensor System with $25lb$ capacity, is used to measure the along and across wind forces and moments. The air velocities in the wake are measured at multiple downstream locations. The experiments are conducted at Reynolds numbers ranging from

$Re = 1.48 * 10^5$ to $Re = 4.73 * 10^5$. Both tree models and the corresponding experimental setup are shown in Fig. 1.

(a) (b) (c) (d)

Figure 1: (a) Lemon tree in open terrain exposure (b) Bending of lemon tree due to wind during test (c) Lemon tree with full foliage (d) Cedar tree with full foliage

2.2. Measurement techniques and instrumentation

The air velocity is measured at five locations on the leeward side of the tree using seven evenly spaced probes as shown in Fig 2. The probe used for measurement is a multi-hole pressure probe capable of resolving all three components of velocity and local static pressure in real time with a frequency response exceeding $2000Hz$. The probe can accurately measure flow fields within an angular range of $\pm 45^o$. Force and moment measurements are recorded using $JR3\ 30E$ multi-axis Force-Torque Sensor System with $25lb$ capacity. Once the flow reaches steady state, the measurements are recorded for a duration of 120 seconds, equivalent to ten minutes at full scale. For frontal area calculation, photographs of each tree configuration are captured using a Nikon camera equipped with an $AF - P\ DX\ 18 - 55\ mm\ f/3.5 - 5.6G\ VR$ lens.

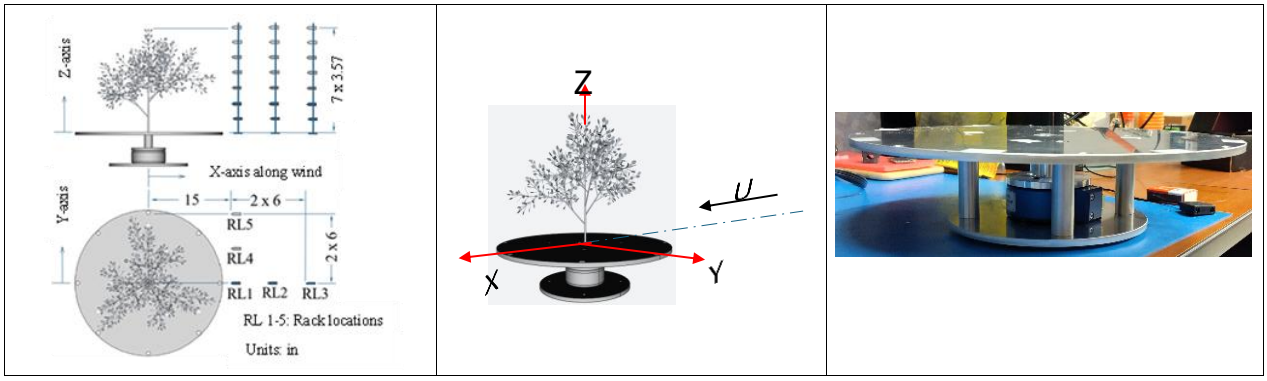

(a) (b) (c)

Figure 2: (a) Probe and rack locations for the measurements (b) Schematic of an isolated tree on force balance with axis system (c) The force balance with mounting plate

3. RESULTS AND DISCUSSION

3.1. Variation of C_d with wind speed and porosity

The current study shows strong influence of tree morphologies on the airflow field. The negative sloped relationship of drag coefficient C_d and crown porosities at a given wind speed U is observed

for both tree configurations. The behaviour of C_d with increasing wind speed for the lemon tree at three different porosity levels is shown in Fig. 3. Porosity of 7% corresponds to the full-foliage or baseline condition, Porosity of 83% represents the defoliated case, while Porosity of 27% depicts a partially foliated or intermediate porosity condition.The frontal silhouette area of the lemon tree is used for all porosity variations, ranging from full foliage or baseline porosity to the defoliated lemon tree. Figure 4 shows the variation of C_d for the Cedar tree model at three porosities of 11%, 25%, and 74%. The porosity nomenclature follows the same scheme as defined earlier. Under the same wind conditions, the Cedar configuration exhibits higher $C_d$values and at higher wind speeds, the drag coefficient exhibits nearly invariant behaviour with increasing wind speed.For the deciduous lemon tree, the relatively greater flexibility and ability to reconfigure depicts that seasonal foliar variations have a stronger impact on the C_d compared to the coniferous Cedar tree. Moreover, lower values of C_d compared to the Cedar tree model might exhibit greater structural rigidity and reduced bending of the Cedar tree models. For the defoliated case in both configurations, C_d shows substantially lower values and invariant behaviour with the wind speed, indicating the importance of leaves in reconfiguration.

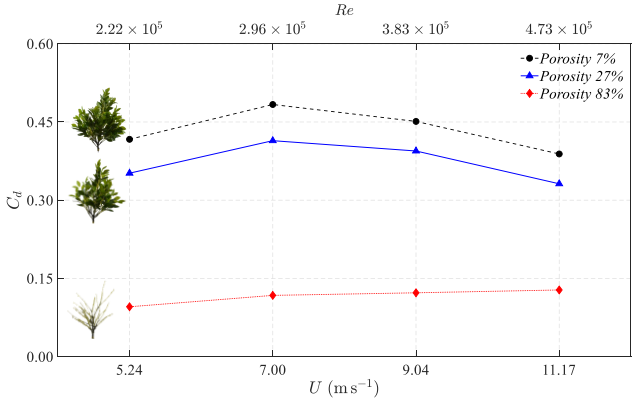

Figure 3: Drag coefficient behaviour with varying wind speeds and porosities for Lemon tree

The behavior of C_d with increasing wind speed for Cedar tree is shown in Fig. 4.

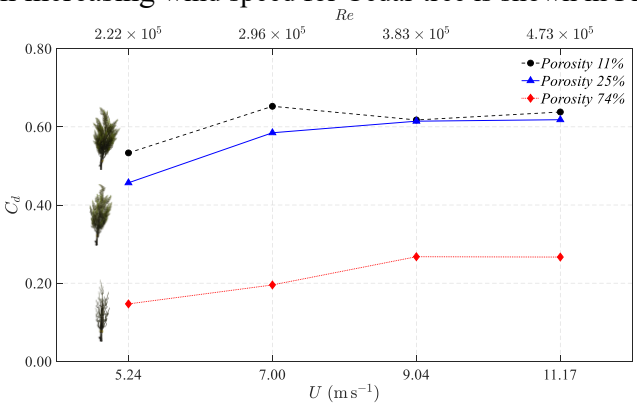

Figure 4: Drag coefficient behaviour with varying wind speeds and porosities for Cedar tree

ACKNOWLEDGEMENTS
The authors would like to acknowledge financial support from the Climate Action and Awareness Fund (CAAF) (grant number: EDF-CA-2021i018) of Environment and Climate Change Canada (ECCC).

4. REFERENCES

J. Cao, Y. Tamura, and A. Yoshida, *"Wind tunnel study on aerodynamic characteristics of shrubby specimens of three tree species,"* J. Wind Eng. Ind. Aerodyn., vol. 11, no. 4, pp. 465–476, 2012, doi: 10.1016/j.ufug.2012.05.003.

C. Gromke, *"A vegetation modeling concept for building and environmental aerodynamics wind tunnel tests and its application in pollutant dispersion studies,"* J. Wind Eng. Ind. Aerodyn., vol. 159, no. 8–9, pp. 2094–2099, Aug. 2011, doi: 10.1016/j.envpol.2010.11.012.

C. Gromke and B. Ruck, *"Aerodynamic modelling of trees for small-scale wind tunnel studies,"* J. Wind Eng. Ind. Aerodyn., vol. 81, no. 3, pp. 243–258, Jul. 2008, doi: 10.1093/forestry/cpn027.

P. F. Grant and W. G. Nickling, *"Direct field measurement of wind drag on vegetation for application to windbreak design and modelling,"* J. Wind Eng. Ind. Aerodyn., vol. 9, no. 1, pp. 57–66, 1998, doi: 10.1002/(SICI)1099-145X(199801/02)9:1<57::AID-LDR288>3.0.CO;2-7.

L. Manickathan, T. Defraeye, J. Allegrini, D. Derome, and J. Carmeliet, *"Comparative study of flow field and drag coefficient of model and small natural trees in a wind tunnel,"* J. Wind Eng. Ind. Aerodyn., vol. 35, pp. 230–239, Oct. 2018, doi: 10.1016/j.ufug.2018.09.011.

L. Manickathan, T. Defraeye, J. Allegrini, D. Derome, and J. Carmeliet, *"Parametric study of the influence of environmental factors and tree properties on the transpirative cooling effect of trees,"* J. Wind Eng. Ind. Aerodyn., vol. 248, pp. 259–274, Jan. 2018, doi: 10.1016/j.agrformet.2017.10.014.

A. Mochida and I. Y. F. Lun, *"Prediction of wind environment and thermal comfort at pedestrian level in urban area,"* J. Wind Eng. Ind. Aerodyn., vol. 96, pp. 1498–1527, 2008.

A. Mochida, Y. Tabata, T. Iwata, and H. Yoshino, *"Examining tree canopy models for CFD prediction of wind environment at pedestrian level,"* J. Wind Eng. Ind. Aerodyn., vol. 96, pp. 1667–1677, 2008.

T. R. Oke, *"Street design and urban canopy layer climate,"* Energy Build., vol. 11, no. 1–3, pp. 103–113, 1988.

Y. Zhao, *"Fluid tunnel research for challenges of urban climate,"* J. Wind Eng. Ind. Aerodyn., Sep. 01, 2023, doi: 10.1016/j.uclim.2023.101659.

Y. Zhao, H. Li, R. Bardhan, A. Kubilay, Q. Li, and J. Carmeliet, *"The time-evolving impact of tree size on nighttime street canyon microclimate: Wind tunnel modeling of aerodynamic effects and heat removal,"* J. Wind Eng. Ind. Aerodyn., vol. 49, May 2023, doi: 10.1016/j.uclim.2023.101528.

C. Wang, Z. H. Wang, K. E. Kaloush, and J. Shacat, *"Perceptions of urban heat island mitigation and implementation strategies: survey and gap analysis,"* J. Wind Eng. Ind. Aerodyn., vol. 66, Mar. 2021, doi: 10.1016/j.scs.2020.102687.